International Journal of Occupational Safety and Ergonomics (*JOSE*) 2006, Vol. 12, No. 1, 43–51

Thermal Performance Assessment of Heat Resistant Fabrics Based on a New Thermal Wave Model of Skin Heat Transfer

Fanglong Zhu
Weiyuan Zhang

College of Fashion, Donghua University, Shanghai, PR China

Guowen Song

Department of Human Ecology, University of Alberta, Edmonton, Alta., Canada

A thermal wave skin model incorporating surface heat flux from a skin simulant sensor is developed to characterize the thermal performance of heat resistant fabrics covering the skin simulant sensor. Comparisons of time to 2nd-degree skin burn and temperature elevation of skin beneath a layer of fabric between the Pennes' equation and the newly developed thermal wave skin model are performed in this research. Results of tolerance time from the Stoll criterion method are also compared with those from 2 skin models in a thermal protective performance calorimeter. It is concluded that the thermal properties of heat resistant fabrics can be characterized more precisely than previously.

thermal performance skin burn skin simulant sensor heat resistant fabrics thermal wave skin model

1. INTRODUCTION

Heat resistant clothing and fabrics protecting against thermal exposure are a crucial requirement in ensuring people's survival and in protecting structures. In many industrial settings, workers face potential exposure to intense radiation heat flux. Exposure may result in skin burns even when heat resistant fabrics or garments are worn. Therefore, the importance of thermal performance of heat resistant fabrics is indisputable, and extensive research work has been done [1, 2, 3, 4, 5, 6]. In the area of fabric evaluation, bench-top tests, thermal mannequin tests and thermal properties test fixture (TPTF) [7] have been developed to estimate thermal protective performance of fabrics or garments under hazard or low heat flux exposure conditions.

In quantitatively estimating thermal performance of fabrics or garments under hazard conditions, time-to-burn damage of skin beneath a layer of fabric is applied using different skin heat transfer models [8, 9, 10, 11]. Nearly all these models have been based on Pennes' skin model [12], which is expressed as

$$\nabla\left(k_{\text{skin}}\nabla T\right)+\omega_{\text{b}}\rho_{\text{b}}C_{\text{p,b}}\left(T_{\text{b}}-T\right)+q_{\text{m}}+q_{\text{r}} = \rho_{\text{skin}}C_{\text{p,skin}}\frac{\partial T}{\partial t}, \quad (1)$$

where ρ_{skin}, $C_{\text{s,skin}}$ and k_{skin} are the density, specific heat and thermal conductivity of human tissue;

Correspondence and requests for offprints should be sent to Fanglong Zhu, College of Fashion, Donghua University, 1882, West Yan'an Road, Shanghai 200051, PR China. E-mail: <pigzhu7979@mail.dhu.edu.cn>.

ρ_b and $C_{p,b}$ are the density and the specific heat of blood and ω_b is blood perfusion rate; q_m and q_r are volumetric heat due to metabolism and spatial heating; T_b is artery temperature and T is human temperature.

Pennes' model inherits some questionable physical and physiological aspects, especially in a short thermal exposure process. In fact, the model is based on the classic Fourier's law, which implies an instantaneous heat flux deposition in skin, i.e., any local temperature disturbance causes an instantaneous perturbation in temperature at each point in medium. But a biological system such as human skin has thermal relaxation time τ for accumulating the thermal energy required for heat transfer to the nearest element within the skin [13].

In the present research, a new testing apparatus with a skin simulant sensor is developed to assess the potential for skin burn injuries and to evaluate the thermal performance of heat resistant fabrics. The heat flux at the surface of the skin simulant sensor determined from temperature elevation of the skin simulant is applied to the thermal wave model of bioheat transfer (TWMBT) for human skin temperature prediction and burn evaluation. The prediction of time to second-degree burn and temperature of skin obtained from the TWMBT model is compared to results obtained by using Pennes' equation.

2. THERMAL WAVE SKIN MODEL

Applying the concept of finite heat transfer velocity, Cattaneo [14] has proposed a modified unsteady heat conduction equation based on Fourier's law integrating thermal relaxation time τ which is

$$q(x, t) + \tau \frac{\partial q}{\partial t} = -k \frac{\partial T}{\partial x}. \tag{2}$$

Based on Equation 2 for heat flux including the characteristic time τ as well as the Pennes' equation, a general form of TWMBT in human skin was introduced by Liu et al. [13] as

$$\nabla[k_{skin} \nabla T] + \left[\omega_b \rho_b C_{p,\,b}(T_b - T) + q_m + q_r + \tau\left(-\omega_b C_{p,b} \frac{\partial T}{\partial t} + \frac{\partial q_m}{\partial t} + \frac{\partial q_r}{\partial t}\right)\right] = \rho_{skin} C_{p,\,skin}\left[\tau\left(\frac{\partial^2 T}{\partial t^2}\right) + \frac{\partial T}{\partial t}\right]. \tag{3}$$

When τ reaches 0, Equation 3 is reduced to the well-known Pennes' bioheat equation based on Fourier's law. Since $\tau \approx 16$–30 s in biological materials, for short heating with its duration comparable to this value, the TWMBT, which accounts for the finite speed of heat transfer, is expected to provide more realistic predictions than those from the traditional bioheat equation.

For practical purposes, 1-D heat transfer is assumed, spatial heating is equal to zero ($q_r = 0$) and steady-state temperature distribution $T_i(x, 0)$ in skin tissue can be written from Equation 3 as

$$k_{skin} \frac{\partial^2 T_i}{\partial x^2} + \frac{\partial k_{skin}}{\partial x} \frac{\partial T_i}{\partial x} + \omega_b \rho_b C_{p,\,b}(T_b - T) + q_m = 0. \tag{4}$$

Subtracting Equation 4 from 3 leads to

$$\rho_b C_{p,\,skin} \frac{\partial^2 \Theta}{\partial t^2} + (\tau \omega_b C_b + \rho_{skin} C_{p,\,skin}) \frac{\partial \Theta}{\partial t} + \omega_b C_b \Theta - k_{skin} \frac{\partial^2 \Theta}{\partial x^2} = q_r, \tag{5}$$

where $\Theta(x, t) = T(x, t) - T_i$ is elevated temperature above steady-state due to heating.

In exposure a surface high heat flux, the corresponding boundary and initial conditions are as follows. Boundary condition at the heating surface, $x > 0$:

$$k_{skin} \frac{\partial \Theta}{\partial x} + q(t) + \tau \frac{\partial q(t)}{\partial t} = 0, \quad 0 < t < t_s, \tag{6}$$

$$k_{skin} \frac{\partial \Theta}{\partial x} = 0, \quad t > t_s. \tag{7}$$

At the blood vessel

$$\Theta(x = L, t) = 0, \quad t > 0. \tag{8}$$

Initial condition, $t = 0$,

$$\Theta(x) = 0, \tag{9}$$

where t_s denotes duration of heating. It is assumed that core temperature at blood vessel was unchanged even if the surface was heated. To numerically calculate the initial steady temperature, skin surface temperature and body core temperature were specified as 32.5 and 37 ^{o}C, respectively. A numerical computation program based on the finite difference method was developed to obtain discrete temperatures in skin.

3. EXPERIMENTAL

3.1. Testing Apparatus

We set up a modified radiant protective performance (RPP) tester (Figure 1) based on the standard on protective clothing and equipment for wildland firefighting [15]. The heat source was provided by thirteen 500-watt quartz tubes. The temperature increase versus time and heat flux was measured using a skin simulant sensor instead of the copper calorimeter located behind the sample fabrics at a distance of 55.4 mm from the surface of the quartz tubes. The heat source was calibrated according to the procedure called for in ASTM F 1939 [16] The skin simulant sensor used an existing procedure for evaluating injuries caused by thermal insults [7]. The technique uses a 12.8-mm thickness glass ceramic block with a thermal conductivity of approximately 1.46 W/m·^{o}C and a thermal diffusivity of approximately 7.3×10^{-7} m^2/s, which responds to heat in a way similar to human skin. The glass ceramic block is attached to a water-cooled plate whose temperature is kept at 37 ^{o}C by a constant-temperature bath. It is instrumented with a thermocouple, which is mounted on the skin simulant surface. A hole is drilled along the normal axis of the sensor to allow the thermocouple wire to be run up inside of the sensor. The thermocouple wires are held on the surface with a heat resistant epoxy-phenolic adhesive. Each thermocouple is connected to a transmitter. A National Instruments (USA) NI 6110 DAQ is used for A/D conversion. A custom designed data acquisition program is produced using the National Instruments LabWindows DACQ development tool.

Typically, the quartz tubes were preheated for 60 s before they were exposed to the fabric samples. Simultaneously, the data acquisition system was activated. The radiant plate temperature was kept unchanged during the whole thermal exposure. The thermal exposure typically lasted between 8 and 25 s, depending on the test requirement and the material being evaluated. After each test, the fabric samples were removed from the apparatus and allowed the cool. The skin simulant sensors were allowed to cool for approximately 15 min, allowing the skin simulant to return to isothermal conditions throughout.

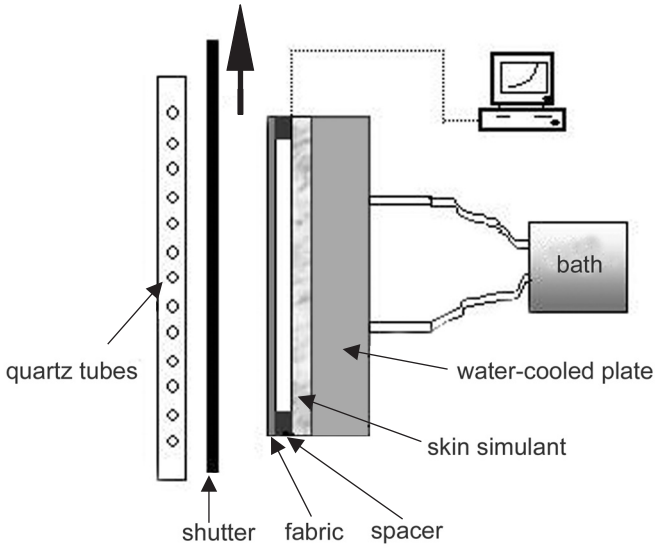

Figure 1. Overall sketch of the experimental system/modified radiant protective performance (RPP) tester.

3.2. Materials and Test Protocol

The basic technical description of fabrics used in the study is provided in Table 1 and 2. All heat resistant fabrics were selected from ZhuHai SRO Ltd. Co. (PR China) and conditioned in (20 ± 2) °C, (65 ± 3)%RH for over 24 hrs before testing.

criterion is based on experimentally observed time to second-degree burn following skin exposure to heat fluxes from 4.2 to 16.8 kW/m^2. However, other data converted into the Stoll curve are obtained through extrapolation. Moreover, the Stoll criterion is strictly valid for constant thermal exposure, for any variation from the shape. Therefore, another integral method proposed by Henriques [17] is

TABLE 1. Physical Properties of Tested Samples

Sample	Material	Structural Feature	Weaving Coefficient (C^1)	Weight (mg/cm^2)	Thickness (mm)	Density (kg/m^3)
A1	Aramid	White twill	—	18.70	0.543	344.4
A2	Panof (fabric)^2	White plain	1.00	35.65	1.200	297.1
A3	Panof (fabric)	White satin	4.00	36.41	0.982	370.8
A4	Panof (fabric)	White crape	1.33	41.32	1.190	347.2

Notes. 1—$C = 2(R_f \bullet R_w)/t_j + t_w$; $R_f(R_w)$—warp(weft) number of within a weave repeat; $t_j(t_w)$—interlacing number between warp and weft within a weave repeat; 2—panof—polyacrylonitrile oxidized fiber.

TABLE 2. Structural Characteristics of Flame Resistant Cotton Fabrics

Sample	Structural Feature	Weight (mg/cm^2)	Thickness (mm)	Density (kg/m^3)	Air Permeability (m^3/min/m^2)	Time to Second-Degree Burn
F1	White plain	24.32	0.502	484.5	150.51	14.2
F2	Yellow plain	23.45	0.567	413.6	135.52	14.6
F3	Yellow plain	21.58	0.481	448.6	155.64	13.1
F4	Yellow plain	26.63	0.615	433.1	170.66	14.2
F5	Yellow plain	22.85	0.504	453.4	159.34	13.5
F6	Yellow plain	23.75	0.543	437.4	118.52	14.3
F7	Yellow plain	18.04	0.446	404.5	185.97	11.9
F8	White twill	20.47	0.458	447.1	176.39	12.8
F9	White twill	24.09	0.521	462.4	174.39	13.1
F10	Knit	21.85	0.482	453.3	200.01	12.2
F11	Gray twill	20.41	0.341	598.5	180.23	11.4
F12	Gray plain	19.63	0.446	440.2	185.24	12.8
F13	Knit	20.05	0.542	369.9	148.62	12.7

3.3. Determination of a Burn Evaluation Criterion

In a burn evaluation, it is regarded that thermal damage begins when the temperature at the basal layer, the interface between the epidermis and dermis, rises above 44 °C [8]. Generally, the Stoll and Chianta curve is used to make estimates of the time it takes for second-degree burn damage to begin to occur for a prescribed exposure. The Stoll

used in conjunction with temperature–time data from a skin simulant sensor to first- and second-degree burns for different level thermal exposure in this research. Henriques found that skin damage could be represented as an integral of a chemical rate process

$$\Omega = \int_0^t P \exp\left(-\frac{\Delta E}{R(T+273)}\right) dt. \qquad (10)$$

P is a constant that varies with skin and local temperature, and ΔE and R are the activation energy and ideal gas constant. Table 3 presents these values developed by Weaver and Stoll [8] providing the best estimation for the time to second-degree burn compared to test data. T is basal layer temperature for first- and second-degree burns while for third-degree burns, it is temperature at the interface between the dermis and the subcutaneous layers. If both conditions of $T > 44\ ^{o}C$ and $\Omega > 0.53$ are satisfied at the basal layer, then a burn is defined as a first-degree one. When $\Omega = 1.0$, a second-degree burn occurs. The integral makes it possible for skin burn to continue in the cooling as well as the heating period.

TABLE 3. Constants for the Second-Degree Burn Integral

Epidermis Temperature	*P* (1/s)	Δ*E*/R
$44 \leq T \leq 50$	2.185×10^{124}	93261.9
$T \geq 50$	1.823×10^{51}	38836.8

Notes. *T*—basal layer temperature, *P*—a constant that varies with skin and local temperature, Δ*E*—activation energy, R—ideal gas constant.

The present research adopts a new skin model rather than the traditional Pennes' model to determine thermal damage to skin. The procedure of determining the degree of skin burn is as follows: the skin simulant sensor is used to determine the heat flux on the skin simulant surface from the elevation of temperature of the surface of the skin simulant, the heat flux data is then applied to the newly developed skin model, and the time to second-degree burn is determined using Henriques Burn Damage Integral [17]. Diller's algorithm [18] is employed to determine the net heat flux q''_{n} at the surface of the skin simulant sensor from the temperature increase of the skin simulant sensor. The elevation in temperature at the skin simulant surface can be measured with the thermocouple bonded to the glass ceramic block surface. At a sample time step t_{n}, q_{n} can be obtained based on the temperature change $(T_i - T_{i-1})$ at all previous time steps, including the one at t_{n}

$$q''_{\mathrm{n}}\ (t_{\mathrm{n}}) = \frac{\sqrt{k\rho C_{\mathrm{p}}}}{\sqrt{\pi \Delta t}} \sum_{i=1}^{\mathrm{n}} \frac{T_i - T_{i-1}}{\sqrt{\mathrm{n} + 1 - j}}. \quad (11)$$

4. RESULTS AND DICUSSION

4.1. Comparison Between TWMBT and Pennes' Equation

With the measurement value of temperature at the skin simulant surface, numerical computation on human skin under Sample A1 of aramid fabric has been conducted for one case in which the prescribed radiant heat flux was 21 kW/m^2. The duration of heating was 10 s and the whole calculating time was 20 s in each experiment. Figure 2 depicts temperature versus tolerance time of skin at 0.08 mm. A substantial deviation can be found between temperature predictions from Pennes' and the TWMBT equations. At the initial stage, Pennes' equation gives higher predictions because it is based on the concept of an instantaneous heat transfer speed inside the skin. On the other hand, the TWMBT equation considers heat transfer in human skin at a finite speed. Therefore, a period of time is needed for the surface heating to travel to a particular point inside the body. The predicted results from both equations coincide at the steady state of human skin after a very long time. In fact, the curves plotted from the numerical skin model calculation data are not so smooth due to the fluctuation in numerically calculated instantaneous incident heat flux at any time step with the use of Diller's algorithm.

Since there exists a distinct difference between temperature predicted by Pennes' and the TWMBT equation, large deviations in skin burns located behind the fabric between these two models can be anticipated. Times for second-degree skin burns for the skin simulant sensor mounting 6 mm behind A1–4 samples are shown in Figure 3. It appears that different burn assessment occurs if the thermal relaxation time τ is considered. The higher the radiant plate temperature, the larger the deviation. Under small heat transfer and when the duration of heating is long, although the difference in the predicted tolerance time and temperature from the two equations will eventually coincide at the end, the difference in the early stage is still distinctive. Thus, for an accurate burn prediction under high heat flux, the TWMBT model

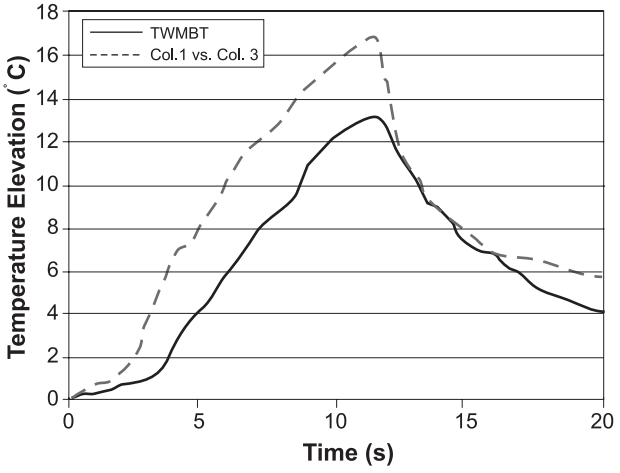

Figure 2. Comparison of temperature changes of skin (TWMBT: τ = 20, Pennes' equation: τ = 0) *Notes.* TWMBT—thermal wave model of bioheat transfer.

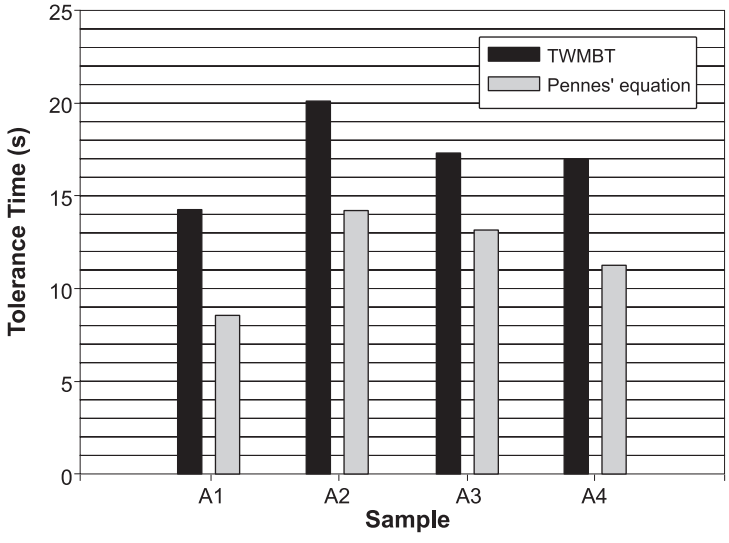

Figure 3. Comparisons of second-degree burn time predictions with Pennes' and the TWMBT equations. *Notes.* TWMBT—thermal wave model of bioheat transfer.

can provide a more realistic tolerance time to second-degree skin burns for estimating thermal performance of heat resistant fabrics.

When examining values of burn time in Table 4, we find that fabrics (A2) with a higher weaving coefficient tend to provide to better thermal protection than ones (A3 and A4) with a lower weaving coefficient with the same weight or thickness due to an increase in tightness with a decrease in the fabric weaving coefficient. But we find that A2 and A3 samples become charred during 8-s thermal exposure when the radiant plate temperature is 600 ^{o}C.

4.2. Comparison With the Stoll Criteria Method

Bench top scale tests require that textile fabrics be exposed to a prescribed fixed radiant exposure. The temperature of the calorimeter is then used to determine the exposure time to cause second-degree burn in accordance with Stoll curves. To provide a rather accurate comparison with the Stoll criterion method, we fabricated a thermal sensor according to the thermal protective performance (TPP) copper calorimeter technique instead of the skin simulant sensor in the RPP tester system. In all the comparative tests, the radiant heat flux was in the same situation of 21 kW/m^2.

TABLE 4. Required Time to Second-Degree Burn of Skin Beneath an Aramid Fabric Layer

	Stoll Criterion Method		TWMBT Model		Pennes' Equation	
Sample	Burn Time t^{I}(s)	*CV* (%)	Burn Time t^{II}(s)	*CV* (%)	Burn Time t^{III}(s)	*CV* (%)
F1	10.4	7.5	14.3	9.5	8.6	9.6
F2	9.9	5.7	14.6	5.8	8.5	6.8
F3	10.2	0.4	13.1	1.1	8.1	1.2
F4	11.2	3.5	14.2	5.4	8.4	5.9
F5	9.6	4.6	13.5	4.6	7.9	5.3
F6	9.8	5.0	14.3	3.0	8.4	4.5
F7	8.5	1.1	11.9	1.7	7.4	4.2
F8	8.7	1.6	12.8	2.0	7.5	3.2
F9	7.6	1.8	13.1	3.1	7.2	1.1
F10	8.1	2.1	12.2	4.8	7.6	5.3
F11	7.2	6.0	11.4	3.6	6.8	4.6
F12	8.1	4.2	12.8	2.3	7.5	2.5
F13	8.3	1.3	12.7	1.9	7.5	1.0

Notes. TWMBT—thermal wave model of bioheat transfer, *CV*—coefficient of variation.

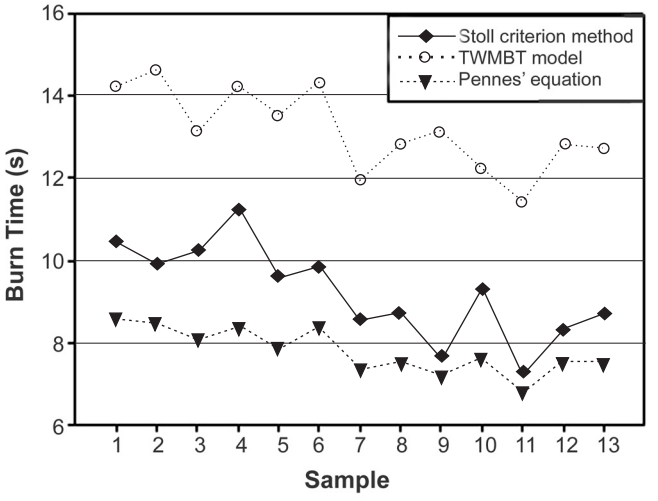

Figure 4. Tolerance time versus sample curve for three methods. *Notes.* TWMBT—thermal wave model of bioheat transfer.

It is shown in Table 4 that none of the *CV* (coefficient of variation, %) values of the three methods are larger than 10%, which means the three methods have good stabilities in thermal performance measurements. Figure 4 indicates that there are distinctive deviations in burn evaluations among the Stoll criterion method and the Henriques burn integral method with the TWMBT and Pennes' model. But there is a good coincidence in shape among the tolerance time of the three methods. Moreover, the good correlation coefficient in Figure 5 between burn time from the Stoll criterion and the Henriques integral with the TWMBT model is .8054, which proves the TWMBT model to be feasible in evaluating thermal performance of heat resistant fabrics.

It is found that burn time values from the Henriques burn integral with the traditional Pennes' is smaller than that from the Stoll criterion due to the difference in the response of the sensors. Namely, the copper disk will not absorb heat in a similar manner to skin. Skin will increase in temperature faster than the copper disk, and this can lead to calculated heat fluxes that may not

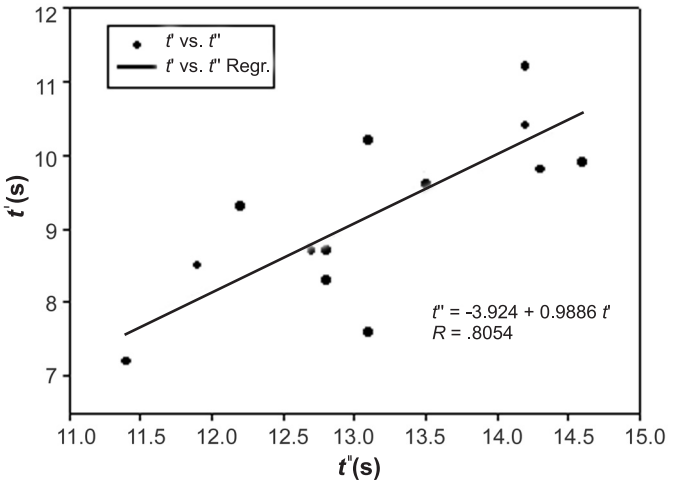

Figure 5. Linear fitting curve between the Stoll method and the Henriques one from the thermal properties test fixture (TWMBT) model. *Notes.* TWMBT—thermal wave model of bioheat transfer.

accurately represent the heat flux to skin for a similar situation.

5. CONCLUSIONS

A new skin model is applied in a study of burn evaluation to assess the thermal performance of heat resistant fabrics and a two-step method including experimental and modeling analysis is introduced to estimate skin burn damage. The skin model has considered the thermal wave effect in a high heat flux incident on skin surface beneath a layer of fabric with a short duration. The higher the heat flux exposure, the more distinctive the deviations between burn evaluations with Pennes' equation and the TWMBT equation. The linear regression of tolerance time to second-degree burn from the Stoll criterion to that from the Henriques burn integral with the TWMBT model shows that there is a good correlation between the two methods.

REFERENCES

1. Lee YM, Barker RL. Thermal protective performance of heat-resistant fabrics in various high intensity heat exposures. Textile Res J. 1987;57(3):123–32.
2. Barker RL, Lee YM. Analyzing the transient thermophysical properties of heat-resistant fabrics in TPP exposures. Textile Res J. 1987;57(6):331–8.
3. Torvi DA. Heat transfer in thin fibrous materials under high heat flux conditions [doctoral dissertation]. Edmonton, Alta., Canada: University of Alberta; 1997.
4. Perkins RM. Insulative values of single-layer fabrics for thermal protective clothing. Textile Res J. 1979;49(4):202–12.
5. Marcelo M. Analysis of thermal performance of two fabrics intended for use as protective clothing. Fire and Materials. 1997;21:115–21.
6. Stuart E, Ron S. The use of modeling in burn injury evaluation beneath clothing layers. Fire and Materials. 1999;23:217–21.
7. Keltner N. Evaluating thermal protective performance testing. Journal of ASTM International (JAI). 2005;2(5).
8. Weaver JA, Stoll AM. Mathematical model of skin exposed to thermal radiation. Aerosp Med. 1969;40:24–30.
9. Killer KR, Hayes LJ. Analysis of tissue injury by burning comparison of in situ and skin flap models. Int J Heat Mass Transfer. 1991;34:1393–406.
10. Mehta AK, Wong F. Summary report from fuels research laboratory. Cambridge, MA, USA: Massachusetts Institute of Technology; 1972.
11. Song GW, Barker R. Comparison of methods used to predict the burn injuries for

performance evaluation of thermal. Journal of ASTM International (JAI). 2005;2(2).

12. Pennes HH. Analysis of tissue and arterial blood temperature in resting human forearm. J Appl Physiol. 1948;1:93–122.
13. Liu J, Chen X, Xu LX. New thermal wave aspects on burn evaluation of skin subjected to instantaneous heating. IEEE Trans Biomed Eng. 1999;46(4):420–8.
14. Cattaneo C. A form of heat conduction equation which eliminates the paradox of instantaneous propagation. Comte Rendus. 1958;247:431–3.
15. National Fire Protection Association (NFPA). Standard on protective clothing and equipment for wildland fire fighting (Standard NFPA 1977; 1993 edition). Quincy, MA, USA: NFPA; 1996.
16. American Society for Testing and Materials (ASTM). Standard test method for radiant protective performance of flame resistant clothing materials (Standard No. ASTM F 1939-99a). West Conshohocken, PA, USA: ASTM; 1999.
17. Henriques FC, Moritz AR. Studies of thermal injury. I. The conduction of heat to and through skin and the temperature attained therein. A theoretical and an experimental investigation. Amer J Pathol. 1947;23: 531–49.
18. Diller TE. Method of determining heat flux from temperature measurement. In: Proceedings of the 42nd International Instrumentation Symposium, Aerospace Industries Division and Test Measurement Division of ISA. San Diego, CA, USA; 1996. vol. 6, p. 231–45.